Quantifying the impact of chronic lead toxicity on the American Bald Eagle *(Haliaeetus leucocephalus)* population in the Great Lakes Region

Christine Brašić[1], Latimer Harris-Ward[2], Gregoire Moreau[3], Carlos Bustamante-Orellana[4] and Jordy Cevallos-Chavez[4]

[1] *University of Wisconsin-Whitewater*
[2] *University of the Pacific*
[3] *Medgar Evers College*
[4] *Arizona State University, Simon A. Levin Mathematical Computational and Modeling Sciences Center*

July 24, 2020

Abstract

An American Icon, the bald eagle, was placed on the endangered species list in 1967 after its population hit critically low levels due to the adverse reproductive effects of DDT. After DDT was banned in 1972, another environmental contaminant continued to affect their recovery—lead. Ingestion of lead-based ammunition was shown to be the eagles' top cause of death, resulting in a 1991 ban of its use for waterfowl hunting. Nearly thirty years later, cases of lead-toxicity in the bald eagle population continue into the present. Noting that the 1991 ban excluded other hunting game, the main source of lead is now linked to the fall and winter big game hunting seasons. This coincides with the eagles' scavenging season, resulting in an annual addition of lead to the eagles' diet. Due to their acidic stomach environment, the eagle is especially lead-free to lead-toxicity. Lead-toxicity may cause severe clinical symptoms (including death), but also more subtle, chronic symptoms. A bald eagle may suffer from chronic toxicity for many years of its life, resulting in continual physiological damage and affected biological mechanisms, including reduced fertility and voracity. Its ecological role as both a scavenger and apex predator make the eagle a valuable resource in the assessment of the Great Lakes ecosystem's health. In order to quantify the impact of lead-contaminated food sources on the bald eagle's population of the Great Lakes, we formulated a system of ordinary differential equations to show the progression through the stages of lead-toxicity and its role in the eagle's population dynamics. We compared the impact of the source of contamination verses treatment of lead-toxicity. We found the bald eagle population is sensitive to its source of lead-contamination.

1 Introduction

The American bald eagle *(Haliaeetus leucocephalus)*, as an apex predator, plays an important ecological role in the in the Laurentian Great Lakes region in the midwestern United States; however the presence of spent lead in the environment causes lead poisoning in bald eagles, which has adverse ecological effects, influencing all parts of the ecosystem. Being an apex predator, the bald eagle establishes ecological stability within the Great Lakes ecosystem. Studies show that the absence of apex predators causes trophic cascades, leading to ecological degradation, and increases the populations of mesopredators [4,14]. This would further degrade the mesopredator-prey dynamics resulting in overhunting and possible extinction of the prey [4]. Other ecological effects include the increase in competition between prey leading to additional extinctions [13]. Additionally, study of contamination of predatory birds is often used to indicate of general contamination of their environment [30].

The ecological effects also directly affect the surrounding communities. About 7% of American farm production occurs in the Great Lakes region. Further, the population is more than 30 million people—roughly 10% of the U.S. population [7]. The Great Lakes also make up 18-21% of the world's freshwater used for drinking and is essential for commercial and recreational fisheries, which when including secondary impacts like lodging, restaurants, and marinas, accounts for over $19 billion dollars in sales and $6.4 billion dollars in revenue for over 250,000 jobs [5, 7, 40].

In 1940, for the first time the Bald Eagle population gained federal protection when Congress passed the Bald Eagle Protection Act. Later, the Protection Act was amended to also include the Golden Eagle [52]. Lead poisoning in eagles is indirectly caused by the use of lead in large game hunting. Many studies show that lead toxicity has been one of the main threats for Bald Eagle population. For instance, Previous studies show that feasting on killed deer constitutes a major source of lead-exposure to scavenging wildlife birds such as Bald Eagles [34, 36, 50].

There are numerous studies concerning lead poisoning in bald eagles that focus on both the the acute and chronic effects of lead toxicity on the bald eagle species [9]. As large birds of prey with opportunistic foraging habits, eagles are easy victims to ingestion of toxins from poisoned or shot carcasses. Data on causes of mortality for 552 Bald and Golden Eagles examined at the National Wildlife Health Center (NWHC) in Madison, Wisconsin, from 1975 through 2013 were published by Russell and Franson (2014). However, it is somewhat difficult to quantify the chronic effects of lead toxicity in bald eagles because their natural depuration rate of lead is 3 weeks [8]. Despite the many articles which explore chronic lead toxicity, [18, 23] and acute effects [21, 45] of lead toxicity, we have yet to encounter a study that mathematically models the population dynamics of the bald eagle population based on lead toxicity levels. This motivates the purpose for the research at hand: using a system of ordinary differential equations constructed from a compartmental model, we successfully quantify the the impact of chronic lead toxicity on the American Bald Eagle (*Haliaeetus leucocephalus*) population in the Great Lakes region by modelling the population dynamics as a function of lead toxicity. By modelling the population dynamics of bald eagles in the Great Lakes using lead

Through numerical simulation, we forecasted the 25 year outlook of the bald eagle population at the current rates of winter food-source contamination to be 35,208 eagles. We then removed the source of contamination to observe the population dynamics in the absence of lead. What we observe is that there is a 1.3% increase (35,638 up from 35,208 bald eagles) in the number of bald eagles when lead is completely removed from the environment. Lastly, we varied the rate by which eagles are retrieved and provided chelation therapy and rehabilitation. As a result, the number of eagles increased by 0.07% (35,221 up from 35,197 bald eagles). Through the use of sensitivity analysis, we were able to identify that the removal of lead from the environment has a greater positive effect on the bald eagle population compared to treating eagles through rehabilitation.

2 Methodology

2.1 Location of Studied Population and the Data Used

We consider eight states which surround the Great Lakes of the United States: Illinois, Iowa, Indiana, Michigan, Minnesota, Missouri, Ohio, and Wisconsin. This region contains north central Wisconsin, which has one of the highest densities of occupied bald eagle nesting territories in North America [31]. Although the bulk of the bald eagle population is contained in the northern states, eagles will migrate and over-winter in the states to the south [43]. Since there exists a correlation between lead-toxicity and lead-accumulation during the winter [1,34,39,44], we found it reasonable to include states to the south. After defining our region, we composed a set of occupied bald eagle nesting territory data obtained from the United States Fish and Wildlife Service (USF&WS), the relevant Departments of Natural Resources (DNRs), and the Center for Biological Diversity [3,6,31,41,48]. Occupied nesting territories are defined as a nest in which an incubating adult, eggs, young, or nest repair is observed [31]. We report our results using total bald eagle population values for the region. In accordance with the USF&WS standards [48], bald eagles over the age of four years constitute 43% of the population, the total population of eagles is obtained through the following calculation:

$$\text{Total Population} = \frac{2}{0.43} * (\text{Number of Occupied Nesting Territories}).$$

2.2 Symbolic Manipulations and Numerical Simulations

For symbolic manipulations, both Mathematica Version 12.1 and Maple (2019) were used for symbolic manipulations [28,33]. For numerical simulations we utilized MATLAB R2019a and R2020a [27] and R version 3.6.1. The data was prepared using R version 3.6.1.

2.3 Assumptions

In order to model the effects of lead-toxicity on the population of bald eagles, we assume lead as the only anthropogenic factor affecting the population. Bald eagles exhibit seasonal scavenging behavior which aligns with the big-game hunting seasons [11, 34, 50]. Considerable studies suggests a strong correlation between lead-based ammunition, hunting seasons, and lead-toxicity in scavenging species [10, 12, 19, 20, 22–24, 36]. Since the 1991 ban of lead-based ammunition for waterfowl hunting, lead-shot contaminated carrion from unretrieved deer is now thought to be the bald eagle's main source of exposure to lead [39,45]. Hence, we assume eagles acquire lead-toxicity through the consumption of lead-contaminated carrion. Carrion is placed, uniformly, into the ecosystem during the annual fall and winter hunting season at a constant rate [38, 50]. Likewise, a uniform distribution of lead in each kilogram of contaminated carrion. Since the population of eagles are also uniformly distributed through the region, they have an equal opportunity to consume contaminated carrion.

We model chronic lead-toxicity by dividing the population into four compartments, with each corresponding to either the population of lead-free eagles, the two-stages of lead-toxicity, or treatment for lead-toxicity. Additionally, the time eagles inhabit each compartment is exponentially distributed and the stages of lead-toxicity are defined by the physiological effects of three ranges of serum-lead-levels. Furthermore, we assume eagles with serum-lead-levels under 0.2 ppm to be lead-free, as these levels are considered background [22].

The first stage of lead-toxicity is defined by eagles with serum-lead-levels between 0.2 to 0.5 ppm. These are classified as eagles with Sub Clinical lead (Pb) Toxicity (SCPT) [22]. We model the subtle, long-term damage of SCPT under the assumption that they exhibit a reduction in fertility and voracity [23, 38]. The second stage of lead-toxicity is defined by eagles with serum-lead-levels of 0.5 ppm and above. These are classified as eagles with Clinical lead (Pb) Toxicity (CPT) [22]. Due to the severity of CPT [37, 39], we assume eagles with CPT either succumb to lead-poisoning or are retrieved and given therapy and rehabilitation. Hence, we assume all non-natural mortality of eagles is due to CPT or failure of CPT treatment. Eagles with CPT do not reproduce and, since CPT is the final stage of lead-toxicity, they do not continue to accumulate lead via the consumption of carrion. If treatment of CPT is successful, these eagles retain lasting physiological damage [15]. Hence, eagles leaving treatment populate the SCPT compartment.

Lead readily binds to calcium, settling in the bones of eagles over time [23]. Lead accumulated within the bones remains stable for long periods of time, but during egg-formation may re-mobilize into

the bloodstream, accumulating in eggshells, allowing for a means of vertical-transfer of lead-toxicity to young [9,10,18,20,49]. For these reasons, we assume eagles with SCPT only beget eagles which also have SCPT and only lead-free eagles beget lead-free eagles. Lastly, we assume a closed ecosystem; the eagle population is not affected by migration. As a consequence of the stated assumptions, in the absence of lead, we assume the population grows logistically.

2.4 Model Formulation

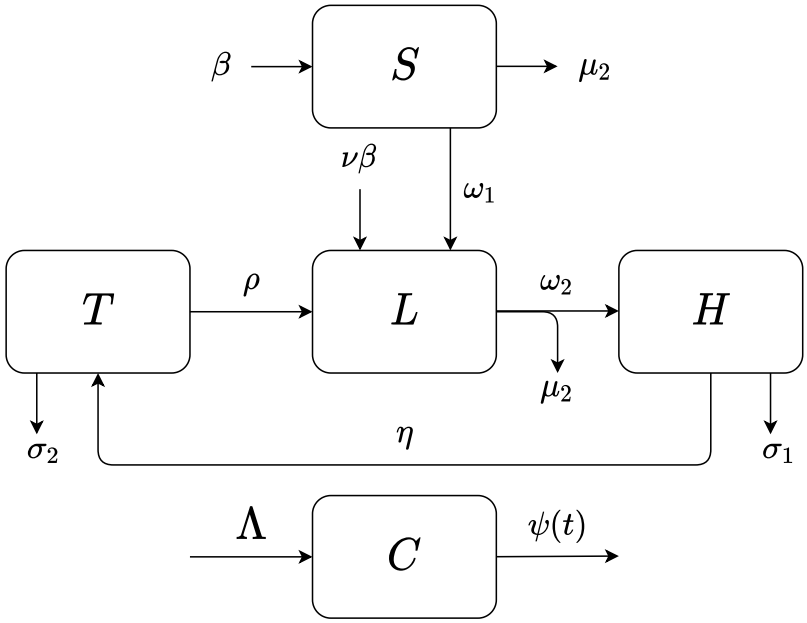

Figure 1: Schematic flow diagram for our mathematical model. The model consists of four compartments: lead-free Eagles (S), SCPT eagles (L), CPT eagles (H), and eagles in treatment (T). Additionally, we consider a state variable for contaminated carrion (C).

1. **Contaminated carrion: C(t)**

   We define contaminated carrion as the source of lead for the bald eagle population. Under assumption, it increases at a constant annual rate, Λ, which represents the yearly amount of unretrieved game containing fragments of spent lead-ammunition. Bald eagles periodically scavenge and gain exposure to lead by consuming the contaminated carrion [34,50]. Eagles may also scavenge uncontaminated carrion, so we divide C by the total yearly level of carrion, M. Both lead-free and SCPT eagles feast upon carrion, at their respective per capita rates (δ_1 and δ_2), reducing the amount in the environment. Carrion also decreases by natural decomposition (at unit rate μ_1). These assumptions lead to the following ODE describing the dynamics of C:

$$\frac{dC}{dt} = \Lambda - \delta_1 \frac{C}{M} S - \delta_2 \frac{C}{M} L - \mu_1 C. \tag{1}$$

2. **Lead-free eagles: S(t)**

   Lead-free (or uncontaminated) eagles increase in number via their natural per capita birth rate, r. Since these eagles are barely or not at all contaminated with lead, they reproduce with unaffected fertility. Their growth rate is logistic, taking into account the entire eagle population (S, L, H, T) with a carrying capacity K for the Great Lakes region. As uncontaminated eagles scavenge contaminated carrion, they become victims of lead toxicity [12]. They move to the SCPT compartment (L) at a per capita ω_1 when all available carrion is contaminated with lead. Lead-free eagles are assumed to be healthy, so they die a natural death (at per capita rate μ_2), not due to lead toxicity.

$$\frac{dS}{dt} = rS\left(1 - \frac{S+L+H+T}{K}\right) - \omega_1 \frac{C}{M} S - \mu_2 S. \tag{2}$$

3. **Eagles with sub-clinical lead toxicity: L(t)**

SCPT eagles have been exposed to lead; their blood contains detectable levels of lead in the range of 0.2 to 0.5 ppm but they do not exhibit clinical symptoms [22]. Although SCPT eagles have no readily observable symptoms of lead-toxicity, they do suffer physiological damage from chronic, sub-clinical serum lead-levels leading to reduced appetite (per capita scavenging rate $\delta_2 = w\delta_1, 0 < w < 1$) and reduced per capita fertility rate ($vr, 0 < v < 1$) [23,38]. SCPT eagles also exhibit logistic growth, but they contribute less to the population of eagles, due to the their damaged fertility. Their offspring are born into the SCPT class due to vertical (maternal) transfer of lead to young [9,10,20,49]. Inflow to the SCPT class comes both from lead-free eagles, at a per capita rate of ω_1, and from eagles leaving treatment, at a per capita rate ρ. Eagles leaving treatment suffer lasting damage and chelation therapy does not reduce their serum lead levels down to zero, hence they flow into the SCPT rather than into the lead-free compartment [15]. Since SCPT eagles have a reduction in appetite and the amount of lead that must be accumulated to move each one of them into the CPT compartment is larger than the amount of lead needed to move a lead-free eagle into the SCPT compartment, it follows that the per capita outflow rate from the SCPT, ω_2, is less than the per capita inflow rate into this compartment, ω_1. SCPT eagles suffer chronic physiological damage, but do not succumb to death via lead toxicity in this compartment, therefore, they only die from natural causes, at per capita rate μ_2.

$$\frac{dL}{dt} = vrL\left(1 - \frac{S+L+H+T}{K}\right) + \omega_1\frac{C}{M}S + \rho T - \omega_2\frac{C}{M}L - \mu_2 L \tag{3}$$

4. **Eagles with clinical lead toxicity: H(t)**

CPT eagles have serum lead-levels high enough (> 0.5 ppm) to exhibit observable signs of lead-toxicity (e.g. difficulty flying, gross lesions on organs, total loss of appetite, etc) [15,23]. SCPT eagles flow into the clinical compartment at a per capita rate ω_2 when all available carrion is contaminated with lead (proportionally reduced by the percentage of lead-contaminated carrion among all available carrion). CPT eagles may succumb to death via lead-toxicity (at per capita rate μ_3), through natural death (at per capita rate μ_2), or they may be retrieved for veterinary care, at a per capita rate η. This retrieval rate moves them to the treatment compartment. Eagles with clinical lead-toxicity are not healthy enough for reproduction. Since we assume eagles at this stage of lead-toxicity either succumb to poisoning or are rescued, they do not interact with contaminated carrion and do not increase their lead-levels.

$$\frac{dH}{dt} = \omega_2\frac{C}{M}L - (\eta + \mu_2 + \mu_3)H, \tag{4}$$

5. **Eagles in treatment: T(t)**

The treatment compartment comprises eagles under veterinary intervention and rehabilitation when exhibiting clinical symptoms of lead-toxicity. CPT eagles flow into the treatment compartment at the per capita rate (at which humans find, capture and treat lead-poisoned eagles), η. Since chelation therapy carries its own risks [15, 37], it is administered until eagles reach sub-clinical or background levels of lead so that, when released, these eagles are not lead-free. Lead-toxicity causes lifelong physiological damage [36], therefore we assume after rehabilitation, they reach sub-clinical biological capacity. Eagles in treatment may die a natural death (at per capita rate μ_2); they may also be euthanized (at per capita rate μ_4). If the eagles survive the treatment and are declared fit, they may be released to join the wild eagle population, at the per capita treatment rate (ρ) [37].

$$\frac{dT}{dt} = \eta H - (\rho + \mu_2 + \mu_4)T, \tag{5}$$

Therefore, our model is given by the following non-linear system of ordinary differential equations:

$$\frac{dC}{dt} = \Lambda - \tau_1 CS - \tau_2 CL - \mu_1 C, \tag{6}$$

$$\frac{dS}{dt} = rS\left(1 - \frac{S+L+H+T}{K}\right) - \omega_1 CS - \mu_2 S, \tag{7}$$

$$\frac{dL}{dt} = vrL\left(1 - \frac{S+L+H+T}{K}\right) + \omega_1 CS + \rho T - \omega_2 CL - \mu_2 L, \tag{8}$$

$$\frac{dH}{dt} = \omega_2 CL - \xi_1 H, \tag{9}$$

$$\frac{dT}{dt} = \eta H - \xi_2 T, \tag{10}$$

where,

$$\tau_1 = \frac{\delta_1}{M}, \quad \tau_2 = \frac{\delta_2}{M}, \quad \xi_1 = \eta + \sigma_1, \quad \sigma_1 = \mu_2 + \mu_3, \quad \xi_2 = \rho + \sigma_2 \text{ and } \sigma_2 = \mu_2 + \mu_4$$

The total eagle population, N, at time t is given by:

$$N(t) = S(t) + L(t) + H(t) + T(t) \tag{11}$$

2.5 Parameter Calculation and Variable Definitions

Under assumption, eagles consume lead through contact with lead-shot-contaminated carrion. Contaminated carrion enter the ecosystem during the annual fall and winter deer-hunting firearm season [53]. Using 2012, 2013, and 2019 deer harvest reports from the region of study [2, 50, 51], along with a 2009 study of Iowa, we estimate an annual harvest rate of 900,000 deer. Studies suggest between ten and 32 percent of deer shot are not retrieved by hunters [34,35,50]. Since data does not account for poaching, discarded offal, and other unreported additions to the overall amount annual deposit of carrion, we use assume 32 percent of deer go unretrieved, giving 280,000 deer per year. Taking the average mass of a deer in Wisconsin, 72 Kilograms [51], we convert the values for total number of unretrieved deer to kilograms and find the constant total mass of carrion, M, is an estimated 20 million Kilograms. To obtain the proportion of lead-contaminated carrion, we use a 2008 study from the US Department of Health and Human Services which found 15 percent of venison donated to Wisconsin food pantries to be contaminated with lead [17]. Assuming the proportion contaminated for food pantry donations is the same proportion of contamination for unretrieved deer, we estimate the input rate of contaminated carrion, Λ, as 3 million Kilograms per year.

A 2009 study of scavengers and animal decomposition in Wisconsin found a deer carcas will remain in the environment for 18 to 55 days during the fall and winter seasons [29]. Adjusting this value to an annual rate and converting deer to Kilograms, we estimate the natural per unit decay rate of carrion, μ_1, as 1 Kilogram per year. Under assumption, carrion will either decay or be consumed by eagles. To obtain consumption rates for bald eagles, we use estimates provided by The American Eagle Foundation. They state a bald eagle averages an annual consumption rate of 219 and 365 pounds [11]. Taking the average mean and converting to Kilograms, we estimate the per capita consumption rate for lead-free eagles, δ_1, as 132 Kilograms per year. We model the physiological effect of chronic lead-toxicity through a reduction in voracity and fertility. Although considerable studies claim a reduction in voracity as a physiological effect of lead-toxicity [16, 22, 23], precise quantification of affected voracity at different stages of lead-toxicity is unknown. We assume a conservative proportion of retained voracity, w, as 0.9. Multiplying this assumed proportion of retained voracity by the per capita consumption rate of lead-free eagles, we estimate the per capita consumption rate of eagles with SCPT, δ_2, as 118.8 Kilograms per year.

Consumption of contaminated carrion serves as a proxy by which eagles accumulate lead, allowing them to traverse the stages of lead-toxicity. The per capita rate for a lead-free eagle to acquire SCPT when all carrion is contaminated, ω_1, is estimated using the annual percent change of lead-free, SCPT, and CPT bald eagles submitted to Iowa wildlife rehabilitation facilities between the years 2007 and 2008 [34]. The annual percent change for the number of eagles with SCPT is estimated as 9.5 percent. Converting this value to the annual rate of change, we estimate the per capita rate by which a lead-free eagle acquires SCPT is 0.100 per year. Similarly, the rate by which an eagle with SCPT acquires CPT,

ω_2, is calculated by first finding the annual percent change for the number of eagles with CPT, 13.2 percent. Converting to the annual rate of change, we estimate the per capita rate by which an eagle with SCPT acquires CPT when all carrion is contaminated is 0.142 per year.

In the absence of lead, we assume the bald eagle population grows logistically. Currently, a clearly defined carrying capacity for the bald eagle of the Great Lakes region does not exist. In 2016, the US Fish and Wildlife Service determined the carrying capacity of the bald eagle, for the entire United States, as $227,800$ [48]. The study concludes an expectation for the growth rate of the population to remain consistent with the growth rate in in 2009. For 2009, according to data contained within the study, the Great Lakes Region contained approximately 20 percent of the country's bald eagle population. Assuming if the average growth rate for the entire country is maintained, then the proportion of eagles in the Great Lakes region is maintained, we set the carrying capacity for the bald eagle of the Great Lakes region of the US, K, to be $46,000$. This study also calculates the annual growth rate in the absence of anthropogenic factors as 0.206. Since we assume lead-toxicity as the only antropogenic factor affecting bald eagles, we use the USF&WS value for the bald eagle population's growth rate, r. Chronic lead-toxicity is shown to damage reproductive organs [15,37], precise values for the reduction in fertility of the bald eagle have not been quantified. Using a 2017 study regarding lead-toxicity induced fertility reduction of Bonelli eagles [20], we make a conservative estimate for the proportion of retained fertility by SCPT eagles, v, to 0.7. To model affected fertility of eagles with SCPT, we multiply our value for the growth rate by the proportion of retained fertility.

Eagles with CPT have considerable long-term physiological damage, including gross ocular, neurological, and cardio lesions [15], along with a weakened bone structure [18]. Due to intraspecific competition [47], we assume bald eagles with CPT are not capable of reproduction. Upon reaching the final stage of lead-toxicity, CPT, eagles die a natural death, die due to lead-poisoning, or are retrieved and provided veterinary care, including chelation therapy and rehabilitation [15,32,34,37]. Since it depends on human intervention, the per capita treatment rate of eagles with CPT, η, functions as a control parameter in the model. We vary this parameter in simulation, but set our initial value by assuming over the course of one year, the probability for an individual eagle with CPT to be found and placed into treatment is 0.5. The majority of eagles with CPT are treated during the hunting season [9,32,50], with chelation therapy and rehabilitation taking anywhere from weeks to months [15,37,38]. Since bald eagles begin courtship and nest construction during the winter [42,43,50], we assume eagles are in treatment during the mating season. Hence, the per capita recovery rate from therapy, ρ, is set to 1 per year. Over the course of a year, approximately 20 percent of eagles in treatment are euthanized [46,54]. Converting this value to an annual rate, we set the per capital death rate due to treatment failure, μ_4 to 0.223.

A summary of all the variables used in the presented model is shown in Table 1. Besides, Table 2 summarizes all the parameters used in the model, along with their units, description, and values.

Table 1: **Variable Definition**

Variable	Description	Units
C	Mass of contaminated carrion	kg
S	Population of lead-free eagles	Non-dimensional
L	Number of eagles with SCPT	Non-dimensional
H	Number of eagles with CPT	Non-dimensional
T	Number of eagles in treatment	Non-dimensional

Table 2: **Parameter Definition**

Parameter	Description	Units	Values[Reference]
Λ	Contaminated carrion input rate	$kg \cdot year^{-1}$	3,000,000 [17]
δ_1	Per capita consumption rate of lead-free eagles	$kg \cdot year^{-1}$	132 [11]
$\delta_2 = w\delta_1$	Per capita consumption rate eagles with SCPT	$kg \cdot year^{-1}$	118.8 [11]
M	Constant total mass of carrion available for consumption	kg	20,000,000 [2, 50, 51]
μ_1	Natural unit decay rate of carrion	$year^{-1}$	1 [29]
μ_2	Natural per capita death rate of eagles	$year^{-1}$	1/30 [11]
μ_3	Lead-induced per capita death rate of eagles	$year^{-1}$	365/133 [22]
μ_4	Per capita death rate of eagles due to treatment failure	$year^{-1}$	0.223 [46]
ω_1	Per capita rate to become SCPT when all carrion is contaminated	$year^{-1}$	0.142 [34]
ω_2	Per capita rate to become CPT when all carrion is contaminated	$year^{-1}$	0.100 [34]
r	Bald Eagle population annual growth rate	$year^{-1}$	0.206 [48]
K	Carrying capacity for bald eagles in the Great Lakes region of the USA	Non-dimensional	46,000 [48]
v	Proportion of retained fertility by SCPT eagles	Non-dimensional	0.7 [20]
w	Proportion of retained voracity by SCPT eagles	Non-dimensional	0.9 [Assumed]
ρ	Per capita recovery rate from therapy	$year^{-1}$	1 [15, 37, 38]
η	Per capita treatment rate of CPT eagles	$year^{-1}$	0.5 [Varied]

3 Analysis

3.1 Positivity of Solutions

We need to prove that the system (6)-(10) supplemented with non-negative initial conditions, has non-negative global solutions. We shall assume, consistently with the concept of carrying capacity, that $N(0) < K$.

First note that the general existence and uniqueness theorem for systems of ODEs ensures that a unique solution exists for $t \in [0, \varepsilon_1]$ for $\varepsilon_1 > 0$ sufficiently small. Next note that as long as the five state variable functions C, S, L, H, T exist, (6) and (7) guarantee that C and S stay positive: in fact, with $g(t) = \tau_1 S(t) + \tau_2 L(t) + \mu_1$ and $G(t) = \int_0^t g(s)ds$, we have

$$C(t) = C(0)e^{-G(t)} + \Lambda \int_0^t e^{G(s)-G(t)} ds \geq 0,$$

and strictly positive if $C(0) > 0$ or $\Lambda > 0$;

$$S(t) = S(0) \exp\left(\int_0^t \left(r\left(1 - \tfrac{S(\tau)+L(\tau)+H(\tau)+T(\tau)}{K}\right) - \omega_1 C(\tau) - \mu_2 \right) d\tau \right) \geq 0,$$

and strictly positive if $S(0) > 0$. Next we would like to prove that

$$L(0), H(0), T(0) \geq 0 \Longrightarrow L(t), H(t), T(t) \geq 0 \text{ for } 0 \leq t \leq \varepsilon_3,$$

if $\varepsilon_3 > 0$ is sufficiently small. Assume from now on that $C(0), S(0) > 0$. The continuity of all functions involved and $T(0) \geq 0$ imply that the source term $\omega_1 C(t)S(t) + \rho T(t)$ in (8) is strictly positive for $0 \leq t \leq \varepsilon_2$, if $\varepsilon_2 > 0$ is sufficiently small. Then, the same argument used for C in (6) applies to prove that $L(t) \geq 0$ on $[0, \varepsilon_2]$. Now that C and L are non-negative on the time-interval $[0, \varepsilon_3]$, where $\varepsilon_3 = \min\{\varepsilon_1, \varepsilon_2\}$, we use the same argument on (9) to show that $H(t) \geq 0$ on $[0, \varepsilon_3]$. Finally, the same argument works now on (10) to establish that $T(t) \geq 0$ on $[0, \varepsilon_3]$.

3.2 Steady State Analysis

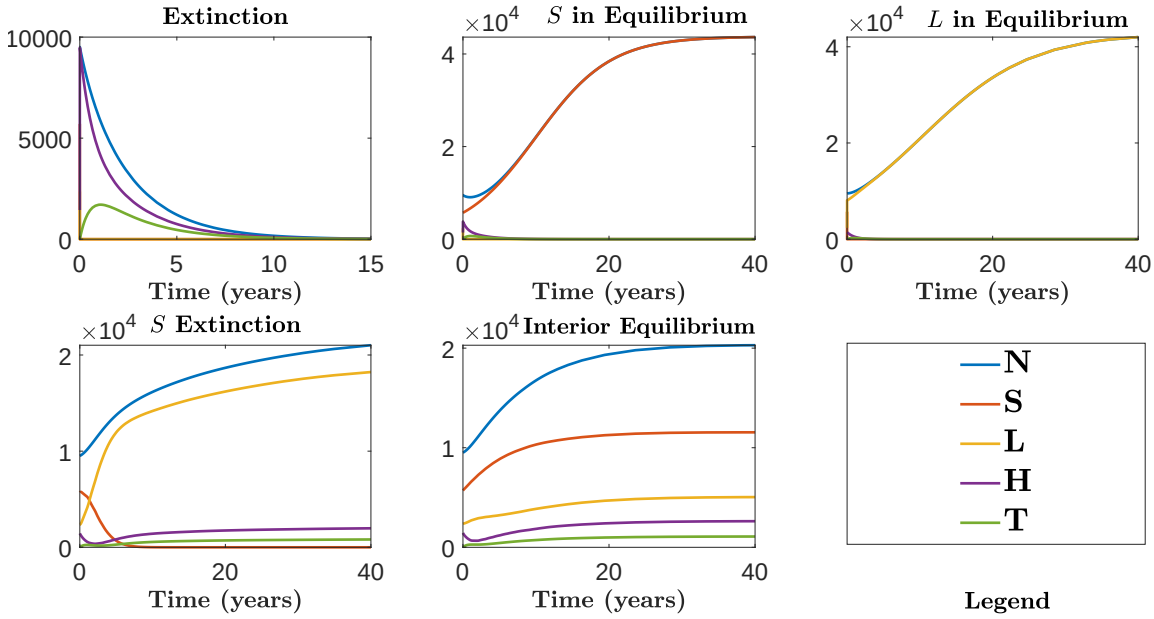

Figure 2: This is a plot of all the equilibrium points that we explicitly find below. Beginning on the first row and starting from left to right, we have $\mathbf{x}_1^*$, $\mathbf{x}_2^*$, $\mathbf{x}_3^*$, $\mathbf{x}_4^*$ and $\mathbf{x}_5^*$ for the fourth panel, and $\mathbf{x}_6^*$.

In order to compute the equilibrium points, we start by setting equations (1)-(5) equal to zero to obtain the following system of linear and quadratic equations.

$$\Lambda - \tau_1 CS - \tau_2 CL - \mu_1 C = 0 \tag{12}$$

$$rS\left(1 - \frac{S+L+H+T}{K}\right) - \omega_1 CS - \mu_2 S = 0 \tag{13}$$

$$vrL\left(1 - \frac{S+L+H+T}{K}\right) + \omega_1 CS + \rho T - \omega_2 CL - \mu_2 L = 0 \tag{14}$$

$$\omega_2 CL - \xi_1 H = 0 \tag{15}$$

$$\eta H - \xi_2 T = 0 \tag{16}$$

By solving the equation (12) for C, we get

$$C^* = \frac{\Lambda}{\tau_1 S^* + \tau_2 L^* + \mu_1}, \tag{17}$$

and solving the equation (13) for S, results in the following two alternative expressions

$$S^* = 0 \tag{18}$$

$$S^* = \frac{K(r - \omega_1 C^* - \mu_2) - r(H^* + L^* + T^*)}{r}. \tag{19}$$

Then, solving the remaining system for each of the state variables gives

$$L^* = \frac{\omega_1 C^* S^* + \rho T^*}{\omega_2 C^* + \mu_2 - vr\left(1 - \dfrac{S^* + L^* + H^* + T^*}{K}\right)} \tag{20}$$

$$H^* = \frac{\omega_2 C^* L^*}{\xi_1} \tag{21}$$

$$T^* = \frac{\eta H^*}{\xi_2} \tag{22}$$

We consider first the equilibrium points with $S^* = L^* = 0$. Substituting these values into equations (21) and (22) we obtain $H^* = T^* = 0$ and then (17) gives $C^* = \frac{\Lambda}{\mu_1} > 0$ (because $\Lambda, \mu_1 > 0$). Therefore, the first equilibrium point (and the only one with $S^* = L^* = 0$) for the system is

$$\mathbf{x}_1^* = (C^*, S^*, L^*, H^*, T^*) = \left(\frac{\Lambda}{\mu_1}, 0, 0, 0, 0\right).$$

Next, we examine the equilibrium points that correspond to $\Lambda = 0$—no input rate of carrion into the environment. It follows from (12) that $C^* = 0$ and then (15) yields $H^* = 0$, and hence (16) implies $T^* = 0$. Now we are left with just the following reduced system of equations, (13)-(14):

$$rS^*\left(1 - \frac{S^* + L^*}{K}\right) - \mu_2 S^* = 0,$$
$$vrL^*\left(1 - \frac{S^* + L^*}{K}\right) - \mu_2 L^* = 0.$$

It is not possible for S^* and L^* to be both nonzero because then we would have $\frac{\mu_2}{r} = \frac{\mu_2}{vr}$, necessitating $v = 1$ when we know that $v < 1$. Thus, one or both of S^* and L^* must be zero. The latter case leads back to the equilibrium x_1^*. The former case, solving this system of equations, leads to two solutions, the first one given by

$$\mathbf{x}_2^* = (C^*, S^*, L^*, H^*, T^*) = \left(0, K\left(1 - \frac{\mu_2}{r}\right), 0, 0, 0\right),$$

and the second one given by

$$\mathbf{x}_3^* = (C^*, S^*, L^*, H^*, T^*) = \left(0, 0, K\left(1 - \frac{\mu_2}{vr}\right), 0, 0\right).$$

These cases are represented in Figure (2) panels (2) and (3), where the population of lead-free eagles (S) and the population of SCPT eagles (L), respectively, grow until they reach their corresponding carrying capacities $K\left(1 - \frac{\mu_2}{r}\right)$ and $K\left(1 - \frac{\mu_2}{vr}\right)$. The equilibrium $\mathbf{x}_3^*$ describes the case where, in the absence of lead, vertical transfer of lead toxicity makes the compartment L persist. To determine the conditions under which $\mathbf{x}_2^*$ exists in the non-negative orthant of the 5-dimensional state space, we must ensure $S^* > 0$. This is the case if the intrinsic per capita growth rate is greater than the natural per capita death rate, that is $r > \mu_2 > 0$. Similarly, to determine the conditions under which $\mathbf{x}_3^*$ exists in the non-negative orthant of the 5-dimensional state space, we must ensure that $L^* > 0$, which is satisfied when $vr > \mu_2$.

Next, we find, $\mathbf{x}_4^*$, $\mathbf{x}_5^*$ and $\mathbf{x}_6^*$, corresponding to the fourth and fifth panels of Figure (2). Let us express C^*, H^*, and T^* in terms of S^* and L^* from equations (12), (15) and (16). In doing so we obtain

$$C^* = \frac{\Lambda}{\tau_1 S^* + \tau_2 L^* + \mu_1}$$
$$H^* = \frac{\omega_2 \Lambda}{\xi_1}\left(\frac{L^*}{\tau_1 S^* + \tau_2 L^* + \mu_1}\right)$$
$$T^* = \frac{\eta \omega_2 \Lambda}{\xi_1 \xi_2}\left(\frac{L^*}{\tau_1 S^* + \tau_2 L^* + \mu_1}\right).$$

By substituting these expressions into equations (13) and (14), we obtain the following system of 2 equations in the 2 state variables, S^* and L^*:

$$\begin{gathered}(((\tau_1 S^* + \tau_2 L^* + \mu_1)(K - L^* - S^*)r - K(\mu_2\tau_2 L^* + \mu_2\tau_1 S^* + \Lambda\,\omega_1 + \mu_1\mu_2))\xi_1 - \omega_2 r\Lambda L^*)\xi_2 - \Lambda\eta\, r\omega_2 L^* = 0 \\ l_3 L^{*3} + l_2 L^{*2} + l_1 L^* + l_0 = 0\end{gathered} \tag{23}$$

Where,

$$\begin{aligned} l_3 &= r v \tau_1 \xi_1 \xi_2, \\ l_2 &= ((v(K\tau_2 + (\tau_1 + \tau_2)S^* + \mu_1)r + K\mu_2\tau_2)\xi_1 + \omega_2 r v \Lambda)\xi_2 + \Lambda\,\eta\, r v \omega_2 \\ l_1 &= \xi_1(v(\tau_1 S^* + \mu_1)(S^* - K)r + K(\mu_2\tau_1 S^* + \omega_2\Lambda + \mu_1\mu_2))\xi_2 - \rho\,\eta\,\omega_2\Lambda\,K \\ l_0 &= -\omega_1\Lambda\,\xi_1\xi_1 K S^*. \end{aligned}$$

By setting $S^* = 0$, we obtain three values for L^*, namely $L^* = 0$ (leading once more to the equilibrium $\mathbf{x}_1^*$) and two nonzero values $L_1^* > L_2^*$ given by

$$L_{1,2}^* = \alpha \pm \beta, \tag{24}$$

where

$$\alpha = \frac{(((K\tau_2 - \mu_1)\,\xi_1 - \omega_2\Lambda)\,vr - K\tau_2\mu_2\xi_1)\,\xi_2 - \Lambda\,\eta\,rv_2}{rv\tau_2\xi_{21}} \tag{25}$$

and

$$\beta = \frac{1}{rv\tau_2\xi_2\xi_1}\left[(rv\Lambda\,(\xi_2+\eta)\,\omega_2)^2 + 2\xi_2\xi_1 vr\omega_2\Lambda\beta_0\right]^{1/2} \tag{26}$$

where,

$$\beta_0 = (((vr - \mu_2 + 2\,\xi_1)\,\xi_2 + \eta\,(vr - 2\,\rho - \mu_2))\,K\tau_2 - rv\mu_1\,(\xi_2+\eta)) + (\xi_1\xi_2\,(K\,(vr-\mu_2)\,\tau_2 + vr\mu_1))^2$$

When $L^* \neq 0$, L_1^* and L_2^* lead to two new equilibria:

$$\mathbf{x}_4^* = \left(\frac{\Lambda}{\tau_2 L_1^* + \mu_1}, 0, L_1^*, \frac{\omega_2\Lambda}{\xi_1}\left(\frac{L_1^*}{\tau_2 L_1^* + \mu_1}\right), \frac{\eta\omega_2\Lambda}{\xi_1\xi_2}\left(\frac{L_1^*}{\tau_2 L_1^* + \mu_1}\right)\right)$$
$$\mathbf{x}_5^* = \left(\frac{\Lambda}{\tau_2 L_2^* + \mu_1}, 0, L_2^*, \frac{\omega_2\Lambda}{\xi_1}\left(\frac{L_2^*}{\tau_2 L_2^* + \mu_1}\right), \frac{\eta\omega_2\Lambda}{\xi_1\xi_2}\left(\frac{L_2^*}{\tau_2 L_2^* + \mu_1}\right)\right),$$

Both of which describe the long-term behavior of panel (4) in Figure (2). When $S^* \neq 0$, then

$$\mathbf{x}_6^* = \left(\frac{\Lambda}{\tau_1 S^* + \tau_2 L^* + \mu_1}, S^*, L^*, \frac{\omega_2\Lambda}{\xi_1}\left(\frac{L^*}{\tau_1 S^* + \tau_2 L^* + \mu_1}\right), \frac{\eta\omega_2\Lambda}{\xi_1\xi_2}\left(\frac{L^*}{\tau_1 S^* + \tau_2 L^* + \mu_1}\right)\right),$$

where S^* and L^* are obtained from solving the system of equations (**??**) and (**??**), giving

$$S^* = -\left(\frac{\xi_1\xi_2\tau_2\mu_2(L^*)^2 + [\xi_1\xi_2((v\omega_1 - \omega_2)\Lambda + \mu_1\mu_2(v-1)) + \eta\omega_2\rho\Lambda]L^*}{\xi_1\xi_2((v\tau_2 - \tau 1)\mu_2 L^* + \omega_2\Lambda)}\right),$$

and L^* is the solution to a cubic equation, providing the possibility of three additional fixed points. However, two of the solutions are complex-valued, so there is only one solution. In order that the last three fixed points be biologically meaningful, they must all be positive. For $\mathbf{x}_4^*$ and $\mathbf{x}_5^*$, as long as $L_1^*, L_2^* > 0$, the equilibrium populations of each compartment will be positive, except for S^*. We can prove this by first separating equations (25) and (26) into smaller expressions, making them easier to analyze, and ignoring the denominator in both because it does not affect the conditions on either α or β. To begin for β, its first and last terms $(rv\Lambda\,(\xi_2+\eta)\,\omega_2)^2$ and $(\xi_1\xi_2\,(K\,(vr-\mu_2)\,\tau_2 + vr\mu_1))^2$, respectively, are both positive because they are both squared. Thus we must show that the second term is positive. We require that $vr - \mu_2 > 2\rho > 0$. Then the following condition

$$(vr - \mu_2 + 2\,\xi_1)\,\xi_2 + \eta\,(vr - 2\,\rho - \mu_2) > \frac{rv\mu_1\,(\xi_2+\eta)}{K\tau_2},$$

satisfies $b > 0$. For a, when the following are true,

$$K > \frac{\mu_1}{\tau_2},$$
$$K\tau_2 - \mu_1 > \frac{\Lambda\omega_2}{\xi_1},$$
$$(K\tau_2 - \mu_1)\xi_1 - \omega_2\Lambda > \frac{K\tau_2\mu_2\xi_1}{vr},$$
$$((K\tau_2 - \mu_1)\xi_1 - \omega_2\Lambda)vr - K\tau_2\mu_2\xi_1 > \frac{\Lambda\eta rv\omega_2}{\xi_2},$$

then $a > 0$. With both $a, b > 0$, then $\mathbf{x}_4^*, \mathbf{x}_5^* > 0$ and we establish that they both exist. For $\mathbf{x}_6^*$, as long as $S^*, L^* > 0$, then the equilibrium corresponding to panel (1) in Figure (2) exists.

Note: Because of the complexity of the cubic equation in L^*, we were unable to perform symbolic analysis to prove the existence of $\mathbf{x}_6^*$. However, using numerical simulations, we find the model supports its existence.

3.3 Stability of Steady States

Determining the stability of the steady states, or equilibrium points, provides us with information as to whether or not the system approaches or avoids the equilibrium points. To do this, we compute the Jacobian matrix, given by

$$J = \begin{bmatrix} -L\tau_2 - S\tau_1 - \mu_1 & -\tau_1 C & -\tau_2 C & 0 & 0 \\ -\omega_1 S & \frac{(K-L-H-2\,S-T)r-K(\omega_1 C+\mu_2)}{K} & -\frac{rS}{K} & -\frac{rS}{K} & -\frac{rS}{K} \\ -\omega_2 L + \omega_1 S & \frac{\omega_1 KC - rvL}{K} & \frac{v(K-2\,L-H-S-T)r-K(\omega_2 C+\mu_2)}{K} & -\frac{rvL}{K} & \frac{-rvL+K\rho}{K} \\ \omega_2 L & 0 & \omega_2 C & -\xi_1 & 0 \\ 0 & 0 & 0 & \eta & -\xi_2 \end{bmatrix},$$

which is a function of the fixed points, and we determine the sign of the eigenvalues. When all eigenvalues are negative, the equilibrium point is stable, and if at least one eigenvalue is positive, then we classify the equilibrium as unstable. The Jacobian evaluated at $\mathbf{x}_1^*$ is

$$\widetilde{\mathcal{J}}(\mathbf{x}_1^*) = \begin{bmatrix} -\mu_1 & -\frac{\tau_1\Lambda}{\mu_1} & -\frac{\tau_2\Lambda}{\mu_1} & 0 & 0 \\ 0 & \frac{(r-\mu_2)\,\mu_1 - \omega_1\Lambda}{\mu_1} & 0 & 0 & 0 \\ 0 & \frac{\omega_1\Lambda}{\mu_1} & \frac{(rv-\mu_2)\,\mu_1 - \omega_2\Lambda}{\mu_1} & 0 & \rho \\ 0 & 0 & \frac{\omega_2\Lambda}{\mu_1} & -\xi_1 & 0 \\ 0 & 0 & 0 & \eta & -\xi_2 \end{bmatrix}.$$

To find the eigenvalues, we determine roots of the characteristic polynomial, given by

$$p_1(\lambda) = \frac{\left((\lambda+\xi_1)\,(\lambda+\xi_2)\,(rv-\lambda-\mu_2)\,\mu_1 - \omega_2\left(\lambda^2 + (\xi_2+\xi_1)\,\lambda + \xi_2\xi_1 - \eta\rho\right)\Lambda\right)\left((r-\lambda-\mu_2)\,\mu_1 - \omega_1\Lambda\right)(\lambda+\mu_1)}{\mu_1^2}.$$

We find that the first two eigenvalues are

$$\begin{aligned} \lambda_1 &= -\mu_1 < 0 \\ \lambda_2 &= \frac{\mu_1(r-\mu_2) - \omega_1\Lambda}{\mu_1} < 0 \quad \text{when} \quad r - \mu_2 > \frac{\omega_1\Lambda}{\mu_1}. \end{aligned}$$

These two eigenvalues are less than zero by definition of our parameters, but we need to obtain the last three eigenvalues from a cubic equation. However, we utilize the Routh test to determine the additional conditions for the stability criterion. The polynomial that we examine is

$$p_{1,a}(\lambda) = \left((\lambda+\xi_1)\,(\lambda+\xi_2)\,(rv-\lambda-\mu_2)\,\mu_1 - \omega_2\left(\lambda^2 + (\xi_2+\xi_1)\,\lambda + \xi_2\xi_1 - \eta\,\rho\right)\Lambda\right) = 0.$$

By expanding $p_{1,a}(\lambda)$ and ordering the terms by degree, we obtain the following Routh array

λ^3	a_0	a_2
λ^2	a_1	a_3
λ^1	$(a_1a_2 - a_0a_3)/a_1$	
λ^0	a_3	

where

$$
\begin{aligned}
a_0 &= \mu_1 \\
a_1 &= (-rv + \mu_2 + \xi_1 + \xi_2)\,\mu_1 + \Lambda\,\omega_2 \\
a_2 &= ((-rv + \mu_2 + \xi_2)\,\xi_1 - \xi_2\,(rv - \mu_2))\,\mu_1 + \omega_2\Lambda\,(\xi_2 + \xi_1) \\
a_3 &= -\xi_2\,(-\Lambda\,\omega_2 + \mu_1\,(rv - \mu_2))\,\xi_1 - \Lambda\,\eta\,\rho\,\omega_2
\end{aligned}
$$

If all $a_i > 0,\ i = 0, 1, 2, 3$, then we must find the conditions where $a_1 a_2 > a_0 a_3$ to ensure that the eigenvalues are negative. To begin, by definition of our parameters, $a_0, a_1 > 0$, because $\mu_1 > 0$ and the sum $\mu_2 + \xi_1 + \xi_2 > rv$. For a_2, we need for $(-rv + \mu_2 + \xi_2)\xi_1 > \xi_2(rv - \mu_2)$, which is again satisfied by our model. The last condition that needs to be satisfied is $a_3 > 0$. For $\mathbf{x}_2^*$, the Jacobian is

$$
\widetilde{\mathcal{J}}(\mathbf{x}_2^*) = \begin{bmatrix}
\frac{(-K\tau_1 - \mu_1)r + K\tau_1\mu_2}{r} & 0 & 0 & 0 & 0 \\
-\frac{\omega_1 K(r - \mu_2)}{r} & -r + \mu_2 & -r + \mu_2 & -r + \mu_2 & -r + \mu_2 \\
\frac{\omega_1 K(r - \mu_2)}{r} & 0 & \mu_2\,(v - 1) & 0 & \rho \\
0 & 0 & 0 & -\xi_1 & 0 \\
0 & 0 & 0 & \eta & -\xi_2
\end{bmatrix},
$$

For $\widetilde{\mathcal{J}}(\mathbf{x}_2^*)$, we find the eigenvalues from the characteristic equation, and the eigenvalues are negative when the following conditions are met,

$$
\begin{aligned}
&\lambda_1 = -\xi_2 = -(\rho + \mu_2 + \mu_4) < 0, \quad \rho, \mu_2, \mu_4 > 0, \\
&\lambda_2 = -\xi_1 = -(\eta + \mu_2 + \mu_3) < 0, \quad \eta \geq 0; \quad \mu_2, \mu_3 > 0, \\
&\lambda_3 = \mu_2(v - 1) < 0, \quad \mu_2 > 0, \quad 0 < v < 1 \\
&\lambda_4 = \mu_2 - r < 0, \quad \mu_2 < r \\
&\lambda_5 = K > \frac{r\mu_1}{\tau_1(r + \mu_2)}, \quad \tau_1, \mu_2, K > 0,
\end{aligned}
$$

thus ensuring that $\mathbf{x}_2^*$ is stable. Likewise, for $\mathbf{x}_3^*$, we find the roots of the characteristic equation of $\widetilde{\mathcal{J}}(\mathbf{x}_3^*)$,

$$
\widetilde{\mathcal{J}}(\mathbf{x}_3^*) = \begin{bmatrix}
\frac{-v(K\tau_2 + \mu_1)r + K\mu_2\tau_2}{rv} & 0 & 0 & 0 & 0 \\
0 & -\frac{\mu_2(v-1)}{v} & 0 & 0 & 0 \\
-\frac{\omega_2 K(rv - \mu_2)}{rv} & -rv + \mu_2 & -rv + \mu_2 & -rv + \mu_2 & -rv + \rho + \mu_2 \\
\frac{\omega_2 K(rv - \mu_2)}{rv} & 0 & 0 & -\xi_1 & 0 \\
0 & 0 & 0 & \eta & -\xi_2
\end{bmatrix},
$$

and we get

$$
\begin{aligned}
&\lambda_1 = -\xi_2 = -(\rho + \mu_2 + \mu_4) < 0, \quad \rho, \mu_2, \mu_4 > 0, \\
&\lambda_2 = -\xi_1 = -(\eta + \mu_2 + \mu_3) < 0, \quad \eta \geq 0, \quad \mu_2, \mu_3 > 0, \\
&\lambda_3 = -\frac{\mu_2(v - 1)}{v} < 0, \quad \mu_2 > 0, \quad 0 < v < 1, \\
&\lambda_4 = -rv + \mu_2, \quad v > 0 \wedge vr > \mu_2, \\
&\lambda_5 = \frac{-Krv\tau_2 - K\mu_2\tau_2 - rv\mu_1}{rv}, \quad \mu_1 > -\frac{K\tau_2(rv + \mu_2)}{rv}
\end{aligned}
$$

where $\lambda_3 > 0$ by definition of v, the proportion of retained fertility of sub-clinical eagles. Thus $\mathbf{x}_3^*$ is an unstable equilibrium. For the last three equilibrium points, $\mathbf{x}_4^*$, $\mathbf{x}_5^*$, and $\mathbf{x}_6^*$, determining the stability is much more difficult, but by substitution of the parameters into the symbolic solver, we find that the equilibrium corresponding to $\mathbf{x}_4^*$ and $\mathbf{x}_5^*$ is unstable whereas the equilibrium for $\mathbf{x}_6^*$ is locally asymptotically stable.

4 Numerical Simulations

For the numerical simulations, we analyze a slightly different model:

$$\frac{dC}{dt} = (\Lambda - \tau_1 CS - \tau_2 CL)\, f(t) - \mu_1 C, \tag{27}$$

$$\frac{dS}{dt} = rS\left(1 - \frac{S+L+H+T}{K}\right) - \omega_1 CS - \mu_2 S, \tag{28}$$

$$\frac{dL}{dt} = vrL\left(1 - \frac{S+L+H+T}{K}\right) + \omega_1 CS + \rho T - \omega_2 CL - \mu_2 L, \tag{29}$$

$$\frac{dH}{dt} = \omega_2 CL - \xi_1 H, \tag{30}$$

$$\frac{dT}{dt} = \eta H - \xi_2 T, \tag{31}$$

where the parameters are the same and

$$f(t) = \begin{cases} 1, & 0 \le t \le 0.25, \\ 0, & 0.25 < t < 1 \end{cases} .$$

We consider this slightly different model to account for changes in the contaminated carrion input rate Λ over the course of the year. The factor $f(t)$ accomplishes this feature. Based on the assumption that bald eagles scavenge during the hunting season, $f(t)$ acts as a switch to signal that during the hunting season, bald eagles scavenge, and during the remaining nine months of the year, the bald eagles do not scavenge at all while the contaminated carrion concurrently decays to zero. We assume that time $t = 0$ begins at the beginning of the hunting season, in November, where the hunting season lasts for three months, or one fourth of the year. The results of the numerical simulations are on the following two pages.

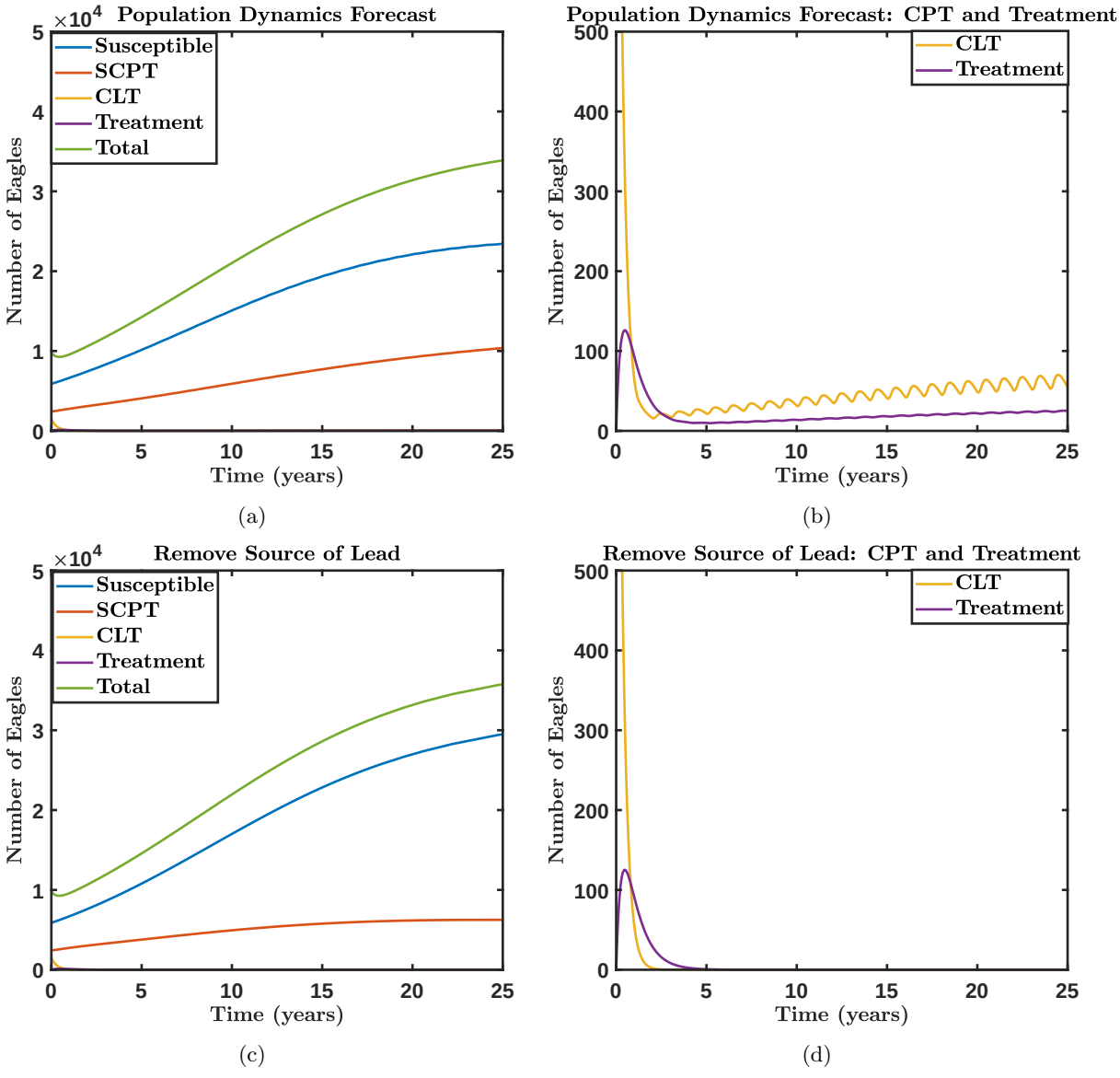

Figure 3: Population dynamics between compartments under current conditions (on the top) and in the absence of further lead-contaminated carrion (bottom).

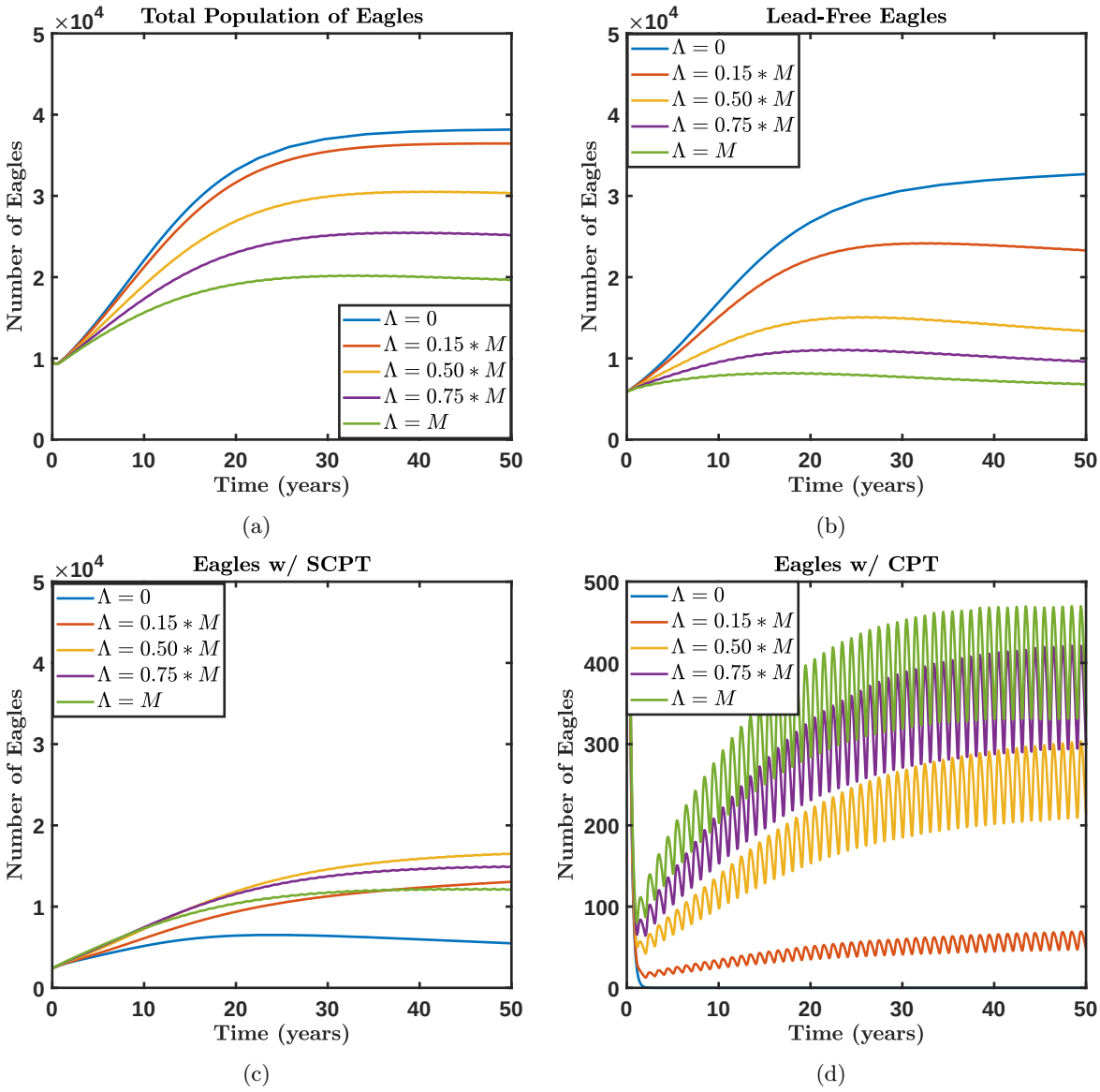

Figure 4: Impact of variations in the annual contaminated carrion input rate, Λ, in the dynamics of the total, lead-free, SCPT, and CPT population sizes of Bald Eagles.

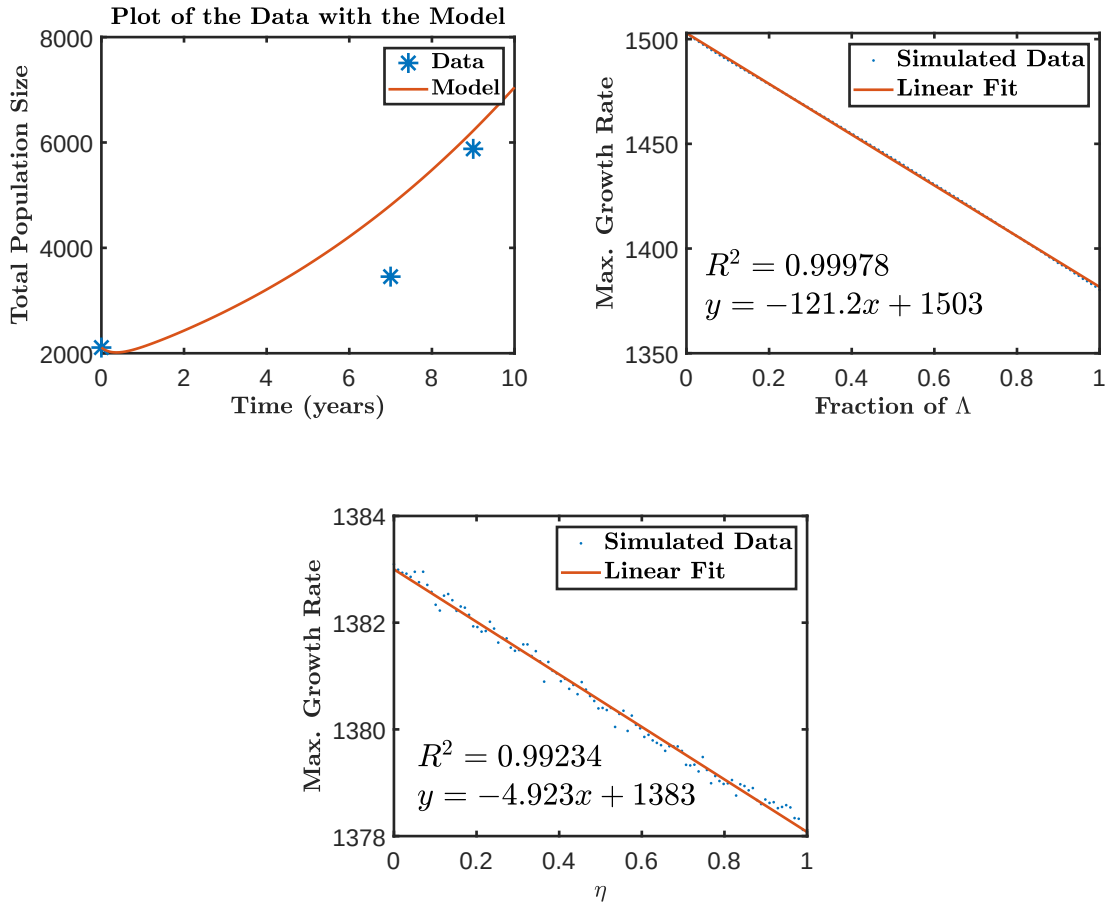

Figure 5: Laurentian Great Lakes region eagles and the total number of eagles from the model (left). The maximum growth rate of the total population as a function of the input rate of carrion, Λ, (right). The maximum growth rate of the total population as a function of the per capita treatment rate of CPT eagles, η, (bottom).

5 Sensitivity Analysis

Based on the analysis in the previous section, we consider the sensitivity indices, or elasticities, of the state variables C, S, L, H, and T with respect to Λ, ω_1, ω_2, and η in order to develop a clearer understanding of how each of these parameters affect each state variable. The sensitivity index SI of some state variable u with respect to a some parameter p is defined by

$$SI_{u_p} := \lim_{\delta p \to 0} \frac{\left(\frac{\delta u}{|u|}\right)}{\left(\frac{\delta p}{|p|}\right)} = \frac{|p|}{|u|}\frac{\partial u}{\partial p} = \frac{|p|}{|u|}u_p.$$

The sensitivity indices describe the percentage by which the state variable increases or decreases when the parameter is increased by one percent.

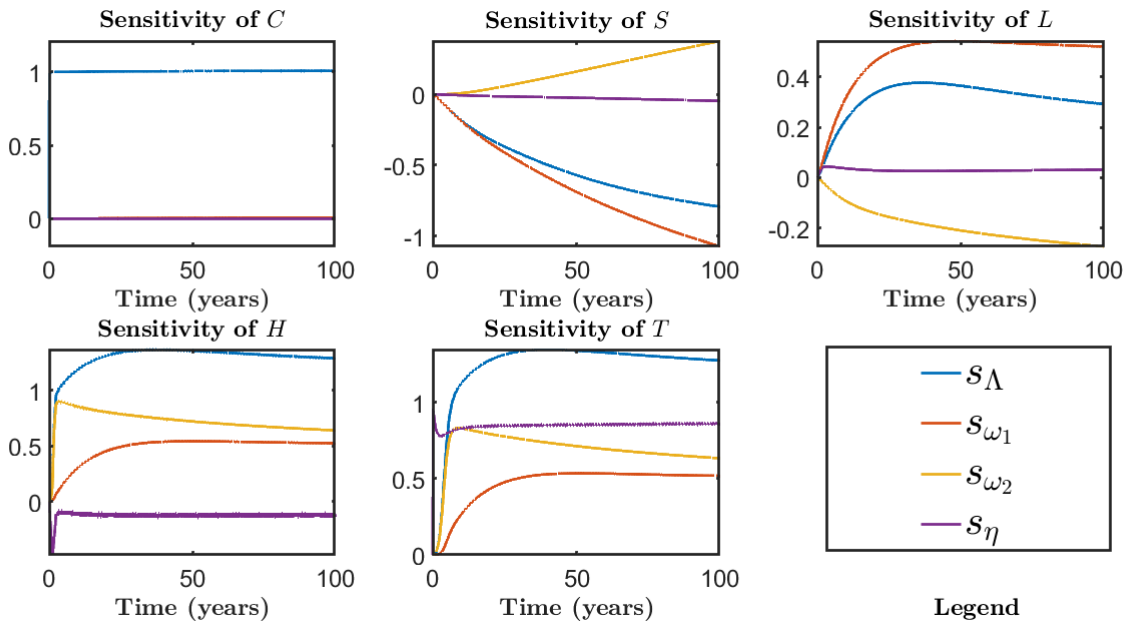

Figure 6: Sensitivity indices of each state variable with respect to the constant rate of the input of carrion (Λ), the per capita rate at which lead-free eagles develop SCPT when all carrion is contaminated (ω_1), the per capita rate at which SCPT eagles develop CPT when all carrion is contaminated (ω_2), and the per capita retrieval rate of eagles for chelation therapy (η).

5.1 The Sensitivity of Carrion

The sensitivity of C is an independent case compared to the other compartments, and we will consider what this means for the S, L, H, and T state variables. Immediately, notice that C is highly sensitive to Λ compared to ω_1, ω_2, and η. Increasing the input rate of contaminated carrion by 1% will increase the amount of carrion by about 1% as expected, compared to close to zero for ω_1, ω_2 and η, all for all time t. C has no explicit dependence on ω_1, ω_2, or η, so the per capita rate at which lead-free eagles develop SCPT when all carrion is contaminated, the per capita rate at which eagles with SCPT develop CPT when all carrion is contaminated, and the retrieval rate have no effect on the amount of the input rate of contaminated carrion in the environment. It is interesting to note that ω_2 has a greater effect on C than ω_1. Again, this is consistent because ω_1 decreases the number of lead-free eagles and increases the amount of eagles with SCPT, resulting in a net loss of contaminated carrion consumption because the latter group has reduced fertility and reduced voracity compared to lead-free eagles.

5.2 The Sensitivity of Lead-Free, SCPT, CPT, and Treated Eagles Compartment Sizes

We first examine the sensitivity indices with respect to the rate at which contaminated carrion enters the environment, Λ. For S, increasing the constant rate of the input of contaminated carrion by 1% decreases S by about 0.8% because as more eagles in S consume contaminated carrion, the faster they develop SCPT. This is also consistent with the sensitivity index for L with respect to Λ because increasing the input of contaminated carrion increases the amount of eagles with SCPT because eagles in S consume more contaminated carrion, raising their lead levels. We see this effect propagate through H and L, which highlights that the entire population is sensitive to Λ. Next, ω_1, the per capita rate at which lead-free eagles develop SCPT, causes a 1% decrease in S and a 0.5% increase in L , H, and T when increased by 1%. As more lead-free eagles consume more contaminated carrion, the more they develop SCPT, which will eventually increase the number of eagles with CPT that are then treated by chelation therapy. The per capita rate at which eagles with SCPT develop CPT where all carrion is contaminated, ω_2, causes increases in S, H, and T along with a decrease in L because eagles with CPT are either treated or succumb effects of lead poisoning. Lastly, an increase in the per capita treatment rate of eagels with CPT η by 1% causes a decrease in S and H and an increase in L and T. This is consistent with what we expect because treated eagles with CPT never fully recover and return to the SCPT class, accounting

for both the decrease in S and H and the increase in L. The T state variable is most sensitive to Λ, followed by η due to the the per capita treatment of eagles with CPT.

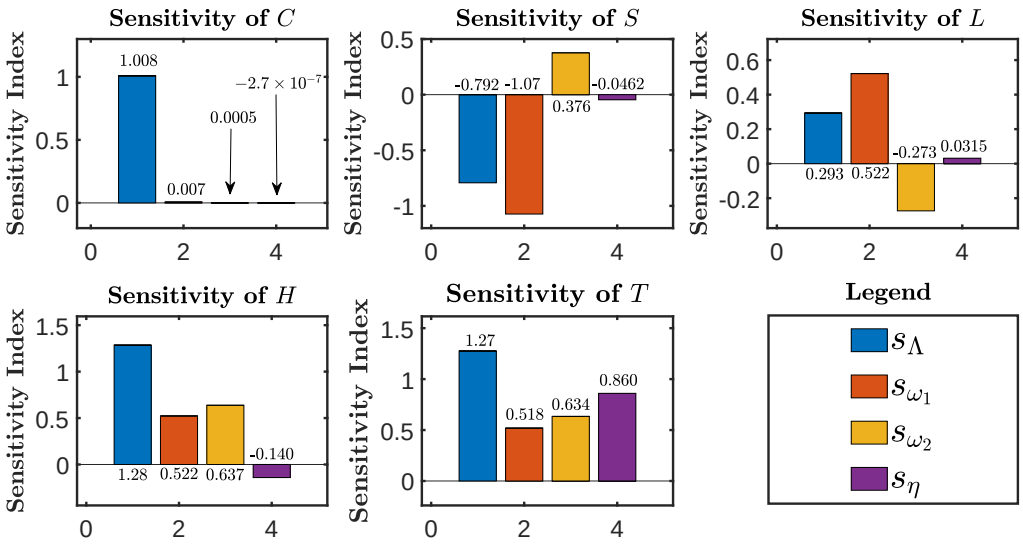

Figure 7: Explicit sensitivity indices of each state variable with respect to Λ, ω_1, ω_2, and η.

6 Discussion

This model contains logistic growth in two compartments: lead-free and SCPT. This allows for the modeling of vertical transfer of lead and its impact on the population's growth. Although this model is primarily compartmental, the novel inclusion of logistic population growth allowed for closer alignment to the 2000, 2007, and 2009 data for the region Figure 4. Since the disease we sought to model, lead-toxicity, is not contagious, the standard dynamics for movement through compartments were not applicable. Hence, we used a fifth equation as a proxy to mobilize eagles through the stages of the disease. In our research, we found it difficult to find a model which not only allows for chronic toxicity of an environmental contaminant, but a precise source. Most models explored only allowed for more general environmental contamination cycle [25, 26].

We sought to explore the relationship between scavenging eagle's consumption of lead-shot contaminated food-sources, using three aspects of chronic exposure: reduction in fertility and appetite, along with the potential to acquire clinical lead-toxicity, resulting in death (in the absence of treatment). We primarily explored the population's sensitivity to the proportion of lead-contaminated carrion (to the total mass of carrion), Λ, and the per capita rate by which eagles are retrieved and placed into treatment, η. We found the population is most sensitive to altering the mass of contaminated carrion. This is expected, due to the long-term physiological damage and increase in per capita death due to lead-toxicity, which is shown in the right plot in Figure (5). In stark contrast, the system has little to no sensitivity with respect to η, except for eagles with CPT that are being treated. We can see that in the bottom plot of Figure (5), we see that as the per capita treatment rate of eagles with CPT decreases, the maximum growth rate of the total population increases, although by a very small amount (a 50% decrease in η results in a 0.14% increase in the maximum growth rate). Although this seems contrary to what is expected, it is completely consistent with the model and its assumptions, particularly the assumption that eagles with SCPT have reduced fertility and voracity. Because eagles with CPT that are treated return to the SCPT class, these eagles consequently have reduced fertility and voracity. Thus, these eagles reproduce at a slower rate compared to healthy lead-free eagles.

This model only considers eagles which succumb to death purely due to lead-toxicity. Research suggests the physiological damages caused by chronic lead toxicity increases the number of deaths due to injury [23, 44]. In recent years, although raptor rehabilitation centers report the prevalence of lead-toxicity cases continues to rise, the main cause of non-natural death of eagles is due to hazards, such as vehicular collision [39]. Typically, these eagles test for elevated serum-lead levels, but the levels are not high enough to definitively assign death to lead-poisoning [44]. Many studies conclude there exists a correlation between deaths due to injuries, such as power-line and vehicle collisions are due to the affected

flight capacity of eagles and disorientation due physiological damage, such as ocular and neurological lesions [15, 16, 34, 39]. In this, our analysis may not encapsulate the entirety of the damage caused by lead-toxicity in the bald eagle population.

Although there is evidence of lead accumulation in eggshells, allowing for vertical-transfer of lead-toxicity to young [9, 10, 49], this does not absolutely imply all young born to eagles with SCPT will also acquire SCPT. For the system's third equilibrium, we observe the number of eagles with SCPT composing the total population of eagles, Figure (2). Although possible, under the model assumptions, in the absence of lead, there does not exist evidence for this phenomena. Future additions to the model could allow eagles with SCPT to beget offspring with background serum-lead-levels, or to allow generational degradation of lead in the population, in the absence of a source.
Although we assume only eagles with CPT are retrieved and given therapy and rehabilitation, in practice eagles with SCPT are given some treatment, such as fluid administration [15]. To more accurately portray the impact of treatment on the population, future works could incorporate treatment of eagles with SCPT.

7 Conclusion

In conclusion, we found that the system is most sensitive to the input rate of carrion Λ. We also found that the system is least sensitive to the per capita treatment rate of CPT eagles. Further, as both Λ and η decrease, the maximum growth rate of the total population increases, with Λ contributing a greater effect. This suggests that the best course of action would be the reduction of lead through preventative measures as opposed to the treatment of CPT eagles. A 50% reduction in the input rate of contaminated carrion resulted in a 4.57% increase in the maximum growth rate of the total population of bald eagles. Likewise, a 50% reduction in η resulted in a 0.14% increase in the maximum growth rate. Although this seems counter-intuitive, this is consistent with the model. Eagles with CPT that are treated do not fully recover even though they are released back into the wild. This is manifested in the fact that eagles with SCPT have reduced fertility and voracity, thus producing a smaller brood of eaglets compared to lead-free eagles.

8 Acknowledgments

We would like to thank Dr. Patrick Kenney, Director and Dr. Fabio Milner, Assistant Director of the Simon A. Levin Mathematical, Computational and Modeling Sciences Center (MCMSC). We would also like to thank Drs. Marlio Paredes and Baltazar Espinoza, co-Directors of the Mathematical and Theoretical Biology Institute (MTBI), as well as coordinators Ms. Rebecca Perlin and Ms. Sabrina Avila, for their efforts in planning and executing the day-to-day activities of MTBI. We also want to give special thanks to Dr. Fabio Milner, Dr. Leon Arriola, Dr. Jose Flores, Carlos Bustamante-Orellana, Jordy Cevallos-Chavez. This research was conducted as part of 2020 MTBI at the Simon A. Levin Mathematical, Computational and Modeling Sciences Center (MCMSC) at Arizona State University (ASU). This project has been supported by the Offices of the Provost and of the Dean of The College of Liberal Arts and Sciences of ASU.

References

[1]

[2]

[3] Bald eagle population exceeds 11,000 pairs in 2007: Long-term trend for each state available for first time.

[4] I want to know about apex predators. http://scienceline.ucsb.edu/getkey.php?key=4532. Accessed: 2020-07-23.

[5] Laurentian Great Lakes. http://www.globalgreatlakes.org/lgl/. Accessed: 2020-07-22.

[6] *Bald Eagle*. 2020.

[7] Environental Protection Agency. Facts and Figures about the Great Lakes. https://www.epa.gov/greatlakes/facts-and-figures-about-great-lakes. Accessed: 2020-07-22.

[8] Bryan Bedrosian, Derek Craighead, and Ross Crandall. Lead exposure in bald eagles from big game hunting, the continental implications and successful mitigation efforts. *PloS one*, 7(12):e51978, 2012.

[9] Jason E. Bruggeman, William T. Route, Patrick T. Redig, and Rebecca L. Key. Patterns and trends in lead (Pb) concentrations in bald eagle (Haliaeetus leucocephalus) nestlings from the western Great Lakes region. *Ecotoxicology*, 27(5):605–618, jul 2018.

[10] Joanna Burger. Heavy metals in avian eggshells: Another excretion method. *Journal of Toxicology and Environmental Health*, 41(2):207–220, 1994.

[11] National Eagle Center. Eagle diet & feeding, 2020.

[12] Luis Cruz-Martinez, Patrick T Redig, and John Deen. Lead from spent ammunition: a source of exposure and poisoning in bald eagles. *Human-Wildlife Interactions*, 6(1):94–104, 2012.

[13] James Estes, Kevin Crooks, and Robert D. Holt. Predators, ecological role of. In Simon A. Levin, editor, *Encyclopedia of Biodiversity*, volume 4, pages 857–878. San Diego: Academic Press, 2001.

[14] James A. Estes, John Terborgh, Justin S. Brashares, Mary E. Power, Joel Berger, William J. Bond, Stephen R. Carpenter, Timothy E. Essington, Robert D. Holt, Jeremy B. C. Jackson, Robert J. Marquis, Lauri Oksanen, Tarja Oksanen, Robert T. Paine, Ellen K. Pikitch, William J. Ripple, Stuart A. Sandin, Marten Scheffer, Thomas W. Schoener, Jonathan B. Shurin, Anthony R. E. Sinclair, Michael E. Soulé, Risto Virtanen, and David A. Wardle. Trophic downgrading of planet earth. *Science*, 333(6040):301–306, 2011.

[15] Jesse A. Fallon, Patrick Redig, Tricia A. Miller, Michael Lanzone, and Todd Katzner. Guidelines for evaluation and treatment of lead poisoning of wild raptors. *Wildlife Society Bulletin*, 41(2):205–211, jun 2017.

[16] J. Christian Franson and Robin E. Russell. Lead and eagles: demographic and pathological characteristics of poisoning, and exposure levels associated with other causes of mortality. *Ecotoxicology*, 23(9):1722–1731, oct 2014.

[17] Jennifer Freed and Alan Yarbrough. Health consultation: The Potential for Ingestion Exposure to Lead Fragments in Venison in Wisconsin. Technical report, U.S. Department of Health & Human Services, Atlanta, GA, 2008.

[18] Laura Gangoso, Pedro Álvarez-Lloret, Alejandro A.B. Rodríguez-Navarro, Rafael Mateo, Fernando Hiraldo, and José Antonio Donázar. Long-term effects of lead poisoning on bone mineralization in vultures exposed to ammunition sources. *Environmental Pollution*, 157(2):569–574, feb 2009.

[19] Kathrin Ganz, Lukas Jenni, Milena M. Madry, Thomas Kraemer, Hannes Jenny, and David Jenny. Acute and Chronic Lead Exposure in Four Avian Scavenger Species in Switzerland. *Archives of Environmental Contamination and Toxicology*, 75(4):566–575, nov 2018.

[20] José M. Gil-Sánchez, Saray Molleda, José A. Sánchez-Zapata, Jesús Bautista, Isabel Navas, Raquel Godinho, Antonio J. García-Fernández, and Marcos Moleón. From sport hunting to breeding success: Patterns of lead ammunition ingestion and its effects on an endangered raptor. *Science of the Total Environment*, 613-614:483–491, feb 2018.

[21] C E Gill and K M Langelier. British columbia. acute lead poisoning in a bald eagle secondary to bullet ingestion. *The Canadian veterinary journal = La revue veterinaire canadienne*, 35(5):303, 1994.

[22] Nancy H. Golden, Sarah E. Warner, and Michael J. Coffey. A review and assessment of spent lead ammunition and its exposure and effects to scavenging birds in the United States. In *Reviews of Environmental Contamination and Toxicology*, volume 237, pages 123–191. Springer New York LLC, Falls Church, VA, 2016.

[23] Hunt W. Grainger. IMPLICATIONS OF SUBLETHAL LEAD EXPOSURE IN AVIAN SCAVENGERS. *Journal of Raptor Research*, 46(4):389–393, 2012.

[24] Susan M. Haig, Jesse D'Elia, Collin Eagles-Smith, Jeanne M. Fair, Jennifer Gervais, Garth Herring, James W. Rivers, and John H. Schulz. The persistent problem of lead poisoning in birds from ammunition and fishing tackle. *The Condor*, 116(3):408–428, aug 2014.

[25] T G Hallam, C E Clark, and G S Jordan. Effects of Toxicants on Populations: A Qualitative Approach II. First Order Kinetics. Technical report, University of Tennessee, Department of Mathematics, 1983.

[26] T.G. Hallam, C.E. Clark, and R.R. Lassiter. Effects of toxicant on population: A Qualitative Approach I. Equilibrium environmental exposure. *Ecological Modelling*, 18(3):291–304, 1983.

[27] The Mathworks, Inc. MATLAB R2020a (Version 9.8) [Computer Software]. Natick, Massachusetts, USA.

[28] Wolfram Research, Inc. Mathematica, Version 12.1 [Computer Software]. Champaign, IL, 2020.

[29] Christopher S. Jennelle, Michael D. Samuel, Cherrie A. Nolden, and Elizabeth A. Berkley. Deer carcass decomposition and potential scavenger exposure to chronic wasting disease. *Journal of Wildlife Management*, 73(5):655–662, 2009.

[30] Martin Lodenius and Tapio Solonen. The use of feathers of birds of prey as indicators of metal pollution. *Ecotoxicology*, 22(9):1319–1334, nov 2013.

[31] Ryan Magana, Austin Dixon, Cala Hakseth, Carly Lapin, Laura Jaskiewicz, Skyler Vold, Joseph Henry, Jake Koebernik, Jim Woodford, Tyler Boudry, Dean Edlin, Rich Staffen, Sharon Fandel, and Ryan Clemo. Wisconsin Bald Eagle and Osprey Nest Surveys 2019. Technical report, Wisconsin Department of Natural Resources, 2019.

[32] Leah K. Manning, Arno Wünschmann, Anibal G. Armién, Michelle Willette, Kathleen MacAulay, Jeff B. Bender, John P. Buchweitz, and Patrick Redig. Lead Intoxication in Free-Ranging Bald Eagles (Haliaeetus leucocephalus). *Veterinary Pathology*, 56(2):289–299, mar 2019.

[33] a division of Waterloo Maple Inc. Maplesoft. Maple (2019) [Computer Software]. Waterloo, Ontario.

[34] Kay Neumann. Bald Eagle Lead Poisoning in Winter. In R. T. Watson, M. Fuller, M. Pokras, and W. G. Hunt (Eds.). Ingestion of Lead from Spent Ammunition: Implications for Wildlife and Humans. 2009.

[35] Charles M Nixon, Lonnie P Hansen, Paul A Brewer, James E Chelsvig, Terry L Esker, Dwayne Etter, Joseph B Sullivan, Robert G Koerkenmeier, and Philip C Mankin. Survival of white-tailed deer in intensively farmed areas of illinois. *Canadian Journal of Zoology*, 79(4):581–588, 2001.

[36] Deborah J. Pain, Rafael Mateo, and Rhys E. Green. Effects of lead from ammunition on birds and other wildlife: A review and update. *Ambio*, 48(9):935–953, sep 2019.

[37] Patrick T. Redig, Lori Arent, Hugo Lopes, and Luis Cruz. Rehabilitation. In David M. Bird, Keith Bildstein, David R. Barber, and Andrea Zimmerman, editors, *Raptor Research and Management Techniques*, chapter 23, pages 411–422. Hancock House, Blaine, WA, 2 edition, 2007.

[38] Patrick T. Redig, Lori Arent, Hugo Lopes, and Luis Cruz. Toxicology. In David M. Bird, Keith Bildstein, David R. Barber, and Andrea Zimmerman, editors, *Raptor Research and Management Techniques*, chapter 23, pages 411–422. Hancock House, Blaine, WA, 2 edition, 2007.

[39] Robin E. Russell and J. Christian Franson. Causes of mortality in eagles submitted to the National Wildlife Health Center 1975-2013. *Wildlife Society Bulletin*, 38(4):697–704, dec 2014.

[40] U.S. Fish & Wildlife Service. Great Lakes Basin Ecosystem Team. https://www.fws.gov/midwest/fisheries/Library/fact-ecoteam.pdf. Accessed: 2020-07-22.

[41] U.S. Fish & Wildlife Service. Bald eagle breeding pairs 1990 to 2006, May 2020.

[42] U.S. Fish & Wildlife Service. Nest chronology of bald eagles in the midwest. https://www.fws.gov/midwest/eagle/Nhistory/NestChron.html#nesting, May 2020.

[43] Stephanie Shepherd. Bald Eagle (Halieetus leucocephalus) status in Iowa, 2019. Technical report, Iowa Department of Natural Resources, Boone, IA, 2019.

[44] Kendall L. Simon, David A. Best, James G. Sikarskie, H. Tyler Pittman, William W. Bowerman, Thomas M. Cooley, and Scott Stolz. Sources of Mortality in Bald Eagles in Michigan, 1986–2017. *Journal of Wildlife Management*, 84(3):553–561, apr 2020.

[45] Erik Stauber, Nickol Finch, Patricia A. Talcott, and John M. Gay. Lead Poisoning of Bald (Haliaeetus leucocephalus) and Golden (Aquila chrysaetos) Eagles in the US Inland Pacific Northwest Region—An 18-year Retrospective Study: 1991–2008. *Journal of Avian Medicine and Surgery*, 24(4):279–287, dec 2010.

[46] Sean M. Strom, Julie A. Langenberg, Nancy K. Businga, and Jasmine K. Batten. Lead Exposure in Wisconsin Birds. Technical report, Wisconsin Department of Natural Resources, Madison, WI.

[47] Courtney Turrin and Bryan D. Watts. Intraspecific intrusion at bald eagle nests. *Ardea*, 102(1):71–78, 2014.

[48] U.S. Fish & Wildlife Service. Bald and Golden Eagles: Population demographics and estimation of sustainable take in the United States, 2016 update; Bald and Golden Eagles: Population demographics and estimation of sustainable take in the United States, 2016 update. Technical report, 2016.

[49] Núria Vallverdú-Coll, Ana López-Antia, Monica Martinez-Haro, Manuel E. Ortiz-Santaliestra, and Rafael Mateo. Altered immune response in mallard ducklings exposed to lead through maternal transfer in the wild. *Environmental Pollution*, 205:350–356, jun 2015.

[50] Sarah E. Warner, Edward E. Britton, Drew N. Becker, and Michael J. Coffey. Bald eagle lead exposure in the Upper Midwest. *Journal of Fish and Wildlife Management*, 5(2):208–216, dec 2014.

[51] Michael A. Watt, Andrew S. Norton, Tim R. Van Deelen, Karl J. Martin, Shelli A. Dubay, Jared F. Duquette, Camille H. Warbington, and Robert E. Rolley. Wisconsin Deer Research Studies, Annual Report 2011-2012. Technical report, Wisconsin Department of Natural Resouces, University of Wisconsin-Madison, Madison, WI, 2012.

[52] Rebecca F. Wisch. Detailed discussion of the bald and golden ealge protection act. *Michigan State University College of Law*, 2002.

[53] Wisconsin Department of Natural Resources. 2019 Wisconsin HUnting and Trapping Seasons. Technical report, Wisconsin Department of Natural Resources, 2019.

[54] Taylor Yaw, Kay Neumann, Linette Bernard, Jodeane Cancilla, Terese Evans, Adam Martin-Schwarze, and Bianca Zaffarano. Lead poisoning in bald eagles admitted to wildlife rehabilitation facilities in Iowa, 2004-2014. *Journal of Fish and Wildlife Management*, 8(2):465–473, dec 2017.